Nondiffractive Subwavelength Wave Beams in a Medium with Externally Controlled Anisotropy

T. Schneider,[1] A. A. Serga,[1] A. V. Chumak,[1] C. W. Sandweg,[1] S. Trudel,[1] S. Wolff,[2] M. P. Kostylev,[3] V. S. Tiberkevich,[4] A. N. Slavin,[4] and B. Hillebrands[1]

[1]*Fachbereich Physik and Forschungszentrum OPTIMAS, Technische Universität Kaiserslautern, 67663 Kaiserslautern, Germany*
[2]*Nano + Bio Center, Technische Universität Kaiserslautern, 67663 Kaiserslautern, Germany*
[3]*School of Physics, M013, University of Western Australia, Crawley, WA 6009, Australia*
[4]*Department of Physics, Oakland University, Rochester, Michigan 48309, USA*

(Received 19 November 2009; published 13 May 2010)

We predict and experimentally demonstrate that in a medium with externally induced anisotropy, a wave source of a sufficiently small size can excite practically nondiffractive wave beams with stable subwavelength transverse aperture. The direction of beam propagation is controlled by rotating the induced anisotropy axis. Nondiffractive wave beam propagation, reflection, and scattering, as well as beam steering have been directly observed by optically probing dipolar spin waves in yttrium iron garnet films, where the uniaxial anisotropy was created by an in-plane bias magnetic field.

DOI: 10.1103/PhysRevLett.104.197203 PACS numbers: 75.30.Ds, 42.25.Fx, 75.30.Gw

A feature common to all types of wave beams is the tendency to increase their transverse aperture, as they propagate, due to unavoidable diffraction within the propagation medium. This effect is especially pronounced when the initial width of the wave beam is comparable with or even smaller than the wavelength of the waves forming the beam. In this work, it is demonstrated that wave beam diffraction can be drastically reduced when waves propagate in a planar medium with a strong induced in-plane anisotropy in which the frequency of propagating waves $f(\mathbf{k}) = f(k_y, k_z)$ strongly depends on the direction of the in-plane wave vector $\mathbf{k} = k_y\mathbf{y}_0 + k_z\mathbf{z}_0$.

In an anisotropic medium, the direction of the wave group velocity $\mathbf{v}_g = 2\pi\partial f(\mathbf{k})/\partial\mathbf{k}$ indicating the direction of energy propagation does not, in general, coincide with the direction of the wave vector $\mathbf{k}$. When the medium's anisotropy is sufficiently strong, the direction of the group velocity of the wave beam may become independent of the wave vectors of the waves forming the beam in the vicinity of a certain carrier wave vector $\mathbf{k}_c$. In such a case, wave packets excited with a broad angular spectrum of wave vectors may be channeled along this direction. The described effect was first observed for phonons propagating in an anisotropic crystal potential [1]. Given the fixed character of the crystallographic anisotropy, the experimentalist cannot control the wave propagation direction. As is shown in this Letter, a similar effect can be used to form and steer practically nondiffractive wave beams that maintain their transverse apertures over large propagating distances. We call them caustic wave beams, in analogy with conventional optics.

In this Letter, dipolar spin waves propagating in yttrium iron garnet (YIG) films are used as an experimental model system for the general concept of controlled caustic wave beam propagation, as was previously suggested [2,3]. In this system the uniaxial symmetry axis is imposed by the magnetization and can thus be controlled by the direction and strength of the bias magnetic field $\mathbf{H}_0$. The frequency $f(\mathbf{k})$ of a propagating spin wave of finite wave vector $\mathbf{k}$ sensitively depends on the relative direction of $\mathbf{k}$ with respect to $\mathbf{H}_0$, providing a mechanism for large angular anisotropy of $f(\mathbf{k})$. This enables an externally controllable, in-plane anisotropic magnetic potential in which the spin waves propagate.

The clear observation of caustic beams in an anisotropic medium requires the excitation of wave packets consisting of many wave components having different in-plane wave vectors, i.e., wave packets with a wide angular spectrum. While the ideal source for such a wave packet is a point source, a source whose size is comparable to (or smaller than) the carrier wavelength of the excited wave packet is also suitable.

In early studies of anisotropic spin-wave propagation in YIG, waves were excited by microstrip antennas having large (several millimeters) apertures [2,4,5]. The angular spectra of the excited waves were thus not sufficiently wide to form caustics. Therefore, only indirect evidence of caustic formation was found, when the excited beam was scattering from a natural defect of the magnetic film (see, e.g., Fig. 6 in [2]).

To overcome these limitations, a novel excitation structure delivering wave packets with wide angular spectra was designed, as shown in Figs. 1(a) and 1(b). A microstrip antenna was used to excite backward volume magnetostatic spin waves [6] into a spin-wave waveguide. The transition between the waveguide and the continuous area of the film acts as an approximate point source [7]. The spin waves propagating in both the waveguide and the continuous area are accessible to probing by space-, time-, and phase-resolved Brillouin light scattering (BLS) spectroscopy [2,8,9], allowing the direct investigation of the excited spin-wave beams. Demidov *et al.* [10] recently

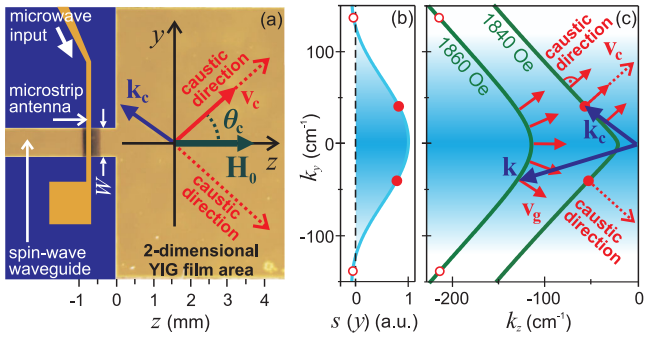

FIG. 1 (color online). (a) Experimental setup. (b) Excitation amplitude of the waveguide antenna as a function of the transverse wave vector k_y ($W = 750$ μm). The shading marks the area were the spin-wave excitation is efficient. (c) Isofrequency curves for different magnetic fields. The dots mark caustic points.

demonstrated that the developed structure can also be used to excite spin-wave beams on the micrometer scale in Permalloy.

A formalism for caustic beam formation in a medium with anisotropic dispersion law $f(\mathbf{k})$ can be developed using the approximate dispersion relation given in [2]. The angle θ which $\mathbf{v}_g$ makes with $\mathbf{H}_0$ is, in general, different at different points of the spectrum, and can be calculated as

$$\theta = \arctan(v_y/v_z) = -\arctan(dk_z/dk_y). \tag{1}$$

Here we taken into account that for a given excitation frequency f_s the dispersion relation can be rewritten as $k_z = k_z(k_y, f_s, H_0)$ and, therefore, the problem can be formally considered as a one-dimensional one.

The resulting isofrequency curves corresponding to bias magnetic fields $H_0 = 1840$ and 1860 Oe are presented in Fig. 1(c). A vector connecting the origin of the coordinate system with any point lying on an isofrequency curve is the wave vector $\mathbf{k}$. The normal to the isofrequency curve shows the local direction of the wave group velocity.

The caustic beams are formed when the direction of group velocity determined by the angle θ is the same for waves having different wave vectors $\mathbf{k}$. This condition can be formulated as $d\theta/dk_y = 0$, or, using Eq. (1),

$$d^2k_z/dk_y^2 = 0. \tag{2}$$

The dots on the isofrequency curves show the points where the curvature (d^2k_z/dk_y^2) is zero. Such points are referred to as caustic points. The vectors $\mathbf{k}_c$ connecting the origin to caustic points are the carrier wave vectors of the caustic wave beams [3].

Figure 1(b) presents the k_y spectrum of spin waves excited by a waveguide antenna of finite width $W = 750$ μm. The shaded area between the first two points of zero amplitude of the spectrum indicates where wave excitation is effective. For the lowest bias magnetic field (1840 Oe), the region of effective wave excitation by the waveguide opening includes the caustic point as well as the approximately linear segment of the isofrequency curve around this point. In contrast, for the larger magnetic field 1860 Oe the caustic points [open red circles in Figs. 1(b) and 1(c)] are situated outside of the region of the effective excitation of the spin waves by the waveguide opening.

On the linear segment of the isofrequency curve corresponding to 1840 Oe, the direction of $\mathbf{v}_g$ is the same for all wave vectors. Thus, a caustic wave beam can form, and the energy of this beam will propagate along the caustic directions perpendicular to the linear segments of the isofrequency curve making the angle θ_c with $\mathbf{H}_0$. The condition (2) defines the carrier wave vector $\mathbf{k}_c$, the group velocity $\mathbf{v}_c$, and the propagation direction θ_c of the caustic beam.

To find the transverse spatial structure (width) of the caustic beam, one can expand the equation of the isofrequency curve k_z (k_y, f_s, H_0) obtained from the approximated dispersion relation in [2] in a Taylor series around $\mathbf{k} = \mathbf{k}_c$ using Eqs. (1) and (2):

$$k_z(k_y) \approx k_{c,z} - \tan\theta_c(k_y - k_{c,y}) + \frac{1}{6}\frac{d^3k_z}{dk_y^3}(k_y - k_{c,y})^3 + \cdots. \tag{3}$$

The spatial profile $a_0(\mathbf{r})$ of the caustic beam created by a pointlike source can be obtained with the help of an inverse Fourier transform as

$$a_0(\mathbf{r}) = \frac{1}{2\pi}\int \exp\{i[k_y y + k_z(k_y, f_s, H_0)z]\}dk_y \approx (\ell_c^2\xi)^{-1/3}\mathrm{Ai}\left(\frac{\eta}{(\ell_c^2\xi)^{1/3}}\right)\cos\theta_c e^{i\mathbf{k}_c\cdot\mathbf{r}}. \tag{4}$$

Here $\mathbf{r}$ is the two-dimensional in-plane position vector, $\xi = z\cos\theta_c + y\sin\theta_c$ is the coordinate along the caustic beam, $\eta = -z\sin\theta_c + y\cos\theta_c$ is the coordinate that is transverse to the axis of the caustic beam, $\mathrm{Ai}(x)$ is the Airy function, and

$$\ell_c = \left(\frac{1}{2}\frac{d^3k_z}{dk_y^3}\right)^{1/2}\cos^2\theta_c \tag{5}$$

is the characteristic length scale of the caustic beam.

Equation (4) gives the spatial profile of the caustic wave beam created by an ideal pointlike source located at the origin ($\mathbf{r} = 0$). The profile of the caustic beam created by a real finite-size source of width W with the amplitude distribution $s(y)$ at $z = 0$ can be calculated as

$$a(\mathbf{r}) = \int_0^W a_0(\mathbf{r} - y\hat{\mathbf{y}})s(y)dy. \tag{6}$$

As is clear from the argument of the Airy function in Eq. (4), the characteristic transverse size of the caustic beam increases with the propagation distance ξ as $(\ell_c^2\xi)^{1/3}$. This, however, applies only to the caustic beams excited by a pointlike source. The real beam, excited by an antenna of finite width, will not spread at all until its

internal width $(\ell_c^2 \xi)^{1/3}$ becomes equal to the width W of the antenna. This condition allows one to estimate the distance of nondiffractive propagation of a caustic wave beam as

$$\xi_c = W^3/\ell_c^2. \tag{7}$$

Compared to the case of a usual diffractive wave beam of finite initial width W (where the characteristic propagation distance is proportional to W^2/ℓ_d, and the characteristic diffractive beam length scale is defined as $\ell_d = |d^2 k_z/dk_y^2|$), the nondiffractive propagation distance of the caustic beam is increased by a factor $W\ell_d/\ell_c^2$ (or, since ℓ_d is usually of the same order of magnitude as ℓ_c, by W/ℓ_c), which is typically much larger than unity. In particular, for the experimental parameters (YIG film thickness is 7.7 μm, magnetic field $H_0 = 1840$ Oe, operation frequency $f_s = 7.132$ GHz, and $W = 750$ μm) used in this Letter, the internal length scale ℓ_c of the caustic beam evaluated from Eq. (5) is $\ell_c = 16.8$ μm. This gives a nondiffractive propagation length of $\xi_c = 1.5$ m.

Note that the carrier wavelength λ of the caustic beam is around 0.96 mm [$k_c = 65.36$ cm^{-1}, Fig. 1(c)] while the width (defined by the width of the waveguide) is 750 μm and significantly smaller than λ, thus creating a subwavelength regime of propagation. Furthermore, the width of the caustic beam is only limited by the width of the waveguide. As it will be shown below (see Fig. 4), a beam width of 400 μm was achieved.

For a bias magnetic field of 1840 Oe [with the caustic point within the excitation region, Fig. 1(b) and 1(c)], two clear wave beams are seen in the BLS intensity map [Fig. 2(a)]. Logarithmic color scaling is used. As expected for a caustic beam, the observed beams are laterally stable, and no diffractive spreading is observed. Figure 2(d) presents the numerically calculated caustic spin-wave beam profiles expected under these experimental conditions. The calculation was based on Huygens' principle using the anisotropic dispersion relation and the excitation amplitude shown in Fig. 1. Comparing Figs. 2(a) and 2(d) demonstrates the very good agreement between the experiment and our model, and unambiguously confirms the observed beams are indeed caustics. Only the reflection of the caustic at the sample's edge was not reproduced numerically, given the calculations were performed for an unbounded space.

To experimentally validate the above approximate theory of caustic beams propagation in an anisotropic medium [Eqs. (4) and (6)], the transverse profile of the caustic beam $a(y)$ at propagation distance $z = 2.5$ mm calculated from Eq. (6) for the initial beam width of $W = 750$ μm was compared with the experimentally measured profile of the caustic beam shown in Fig. 2(a). The results of this comparison are presented in Fig. 3(a). It is clear that the approximate analytic theory of Eq. (6) gives a good quantitative description of the experiment. The fine transverse structure seen in the analytical calculation for a point-source excitation [Fig. 3(b)] and caused by the interference between waves with different wave vectors inside the caustic beam is substantially suppressed when the beam has a finite width ($W = 750$ μm). As Fig. 3 also shows, the signal-to-noise ratio of the experiment is not sufficient to resolve this structure.

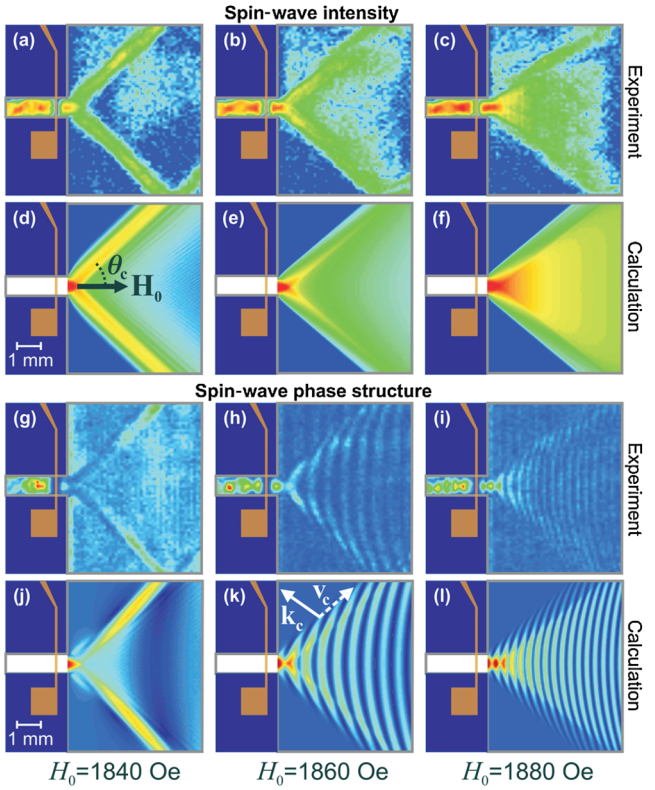

FIG. 2 (color online). Measured and calculated intensity and phase profiles of the propagating spin-wave beams for different magnetic fields. (a)–(c) Measured spin-wave intensity profiles. (d)–(f) Calculated profiles. (g)–(i) Measured spin-wave phase profiles. (j)–(l) Calculated phase profiles. The relative direction of the caustic beam carrier wave vector $\mathbf{k}_c$ and group velocity $\mathbf{v}_c$ are explicitly shown in (k). ($W = 750$ μm, $f_s = 7.132$ GHz).

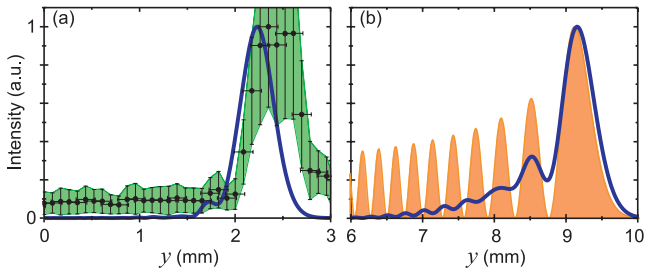

FIG. 3 (color online). Transverse spatial profiles $|a(y)|^2$ of caustic wave beams. (a) Caustic beam excited by a 750 μm wide waveguide at the distance $z = 2.5$ mm from it: dots with shading, BLS experiment Fig. 2(a); solid line, theoretical calculation using Eq. (6). (b) Caustic beam excited by an ideal point source (shading) and by a 750 μm wide waveguide (solid line) at the distance $z = 0$ mm.

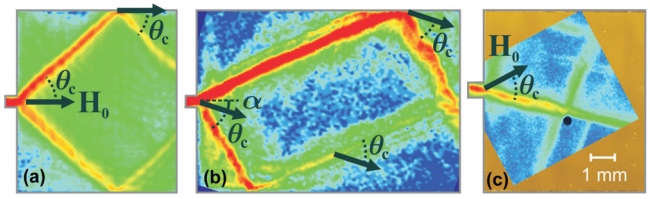

FIG. 4 (color online). Scattering of caustic beams from the medium boundaries (a),(b) and a defect (black dot) (c). Conditions: $H_0 = 1860$ Oe, $f_s = 7.132$ GHz, and $W = 400$ μm (a),(b) and 500 μm (c).

As it has been mentioned, efficient caustic beam formation cannot happen if the curvature of the isofrequency curve is nonzero through the range of efficient spin-wave excitation. This is the case for the higher magnetic fields studied here. For example, for $H_0 = 1860$ Oe, the caustic point lies beyond the range of efficient excitation [see Fig. 1(b)]. While still possible, caustic beam formation is strongly hindered. Thus for higher bias fields, both experiment [Figs. 2(b) and 2(c)] and numerical calculations [Figs. 2(e) and 2(f)] indicate that the caustic beams become less pronounced.

Figures 2(g)–2(i) show the measured phase structure of the propagating spin waves. The measurements have been performed by phase-resolved BLS [8,9]. One sees the spin-wave wave fronts visualized through constructive and destructive interference between the spin-wave signal and a reference signal having constant phase. The results of the numerical calculation of the spin-wave phase fronts are shown in Figs. 2(j)–2(l). Within the caustic beams the wave fronts are not perpendicular to the beam direction, since the wave vector $\mathbf{k}_c$ and the group velocity $\mathbf{v}_c$ are not collinear [see Fig. 2(k)]. One can also see that for $H_0 = 1840$ Oe, where caustic formation was clearly observed in the intensity image, the distance between phase fronts (i.e., the wavelength) is clearly larger than the transverse aperture [only one wave front is observed in Fig. 2(g)].

The unique relation between caustic wave beam propagation and the axis of anisotropy was further explored. Figure 4(a) demonstrates the scattering of caustic spin-wave beams from the YIG film boundaries when $\mathbf{H}_0$ is directed along these boundaries. The boundary region from which the propagating caustic wave beam scatters acts as a secondary wave source, whose finite size is of the order of the beam's width. This secondary source also radiates a wave packet with a wide angular spectrum that again forms caustic wave beams propagating at the same angle θ_c to the anisotropy axis defined by $\mathbf{H}_0$ as the initial caustic wave beam.

At first glance it might seem that the reflection of the caustic at the medium boundary follows the laws of geometric optics, as the incident and reflection angles are equal. However, as we rotate the bias magnetic field clockwise through the angle $\alpha = 20°$ to be inclined with respect to the medium boundary, the pattern of the beam reflection at the boundary drastically changes [see Fig. 4(b)]. First, since the angular spectrum of the initial wave packet is tilted, the amplitudes of the upper and lower caustic beams are now substantially different. Second, and more importantly, the incidence and reflection angles of the propagating caustic are no longer equal. Indeed, the direction of the secondary, reradiated wave beam is determined by the direction of the inclined anisotropy axis in the medium $\mathbf{H}_0$.

A similar effect is seen in Fig. 4(c), where the bias magnetic field was rotated counterclockwise by 30°, to directly aim the caustic beam at the intentionally made defect in the film (shown as a black dot). It is clear from Fig. 4(c) that, as in Figs. 4(a) and 4(b), scattering of the caustic beam from the defect creates a secondary finite-sized source that excites caustic beams propagating at the same angle with respect to the anisotropy axis $\mathbf{H}_0$, preserving their transverse aperture through propagation. It should be pointed out that the defect reradiates caustic beams in all four possible directions.

In conclusion, it is demonstrated that a narrow wave source excites caustic spin-wave beams with a stable transverse aperture which can be subwavelength. These caustic beams propagate and scatter along well-defined directions that can be controlled by rotating the medium's anisotropy axis by orienting an externally applied field. These results are useful not only for the fundamental understanding of spin-wave propagation, but can also easily transfer to any wave in a strongly anisotropic medium.

This work was supported by the DFG (Graduiertenkolleg 792 and Grant No. SE 1771/1-1), the Australian Research Council, the National Science Foundation (Grant No. ECCS 0653901), the U.S. Army TARDEC, RDECOM (Contract No. W56HZW-09-P-L564), and the AvH foundation (S. T.).

[1] B. Taylor, H. J. Maris, and C. Elbaum, Phys. Rev. Lett. **23**, 416 (1969).
[2] O. Büttner *et al.*, Phys. Rev. B **61**, 11 576 (2000).
[3] V. Veerakumar and R. E. Camley, Phys. Rev. B **74**, 214401 (2006).
[4] F. A. Pizzarello, J. H. Collins, and L. E. Coerver, J. Appl. Phys. **41**, 1016 (1970).
[5] A. B. Valyavsky, A. V. Vashkovsky, A. V. Stal'makov, and V. A. Tyulyukin, Sov. Tech. Phys. Lett. **34**, 616 (1989).
[6] R. W. Damon and J. R. Eshbach, J. Phys. Chem. Solids **19**, 308 (1961).
[7] T. Schneider, A. A. Serga, C. Sandweg, and B. Hillebrands, in *Proceedings of the 52nd Annual Conference on Magnetism and Magnetic Materials, Tampa, FL, 2007*, Abstract No. ER-05.
[8] A. A. Serga, T. Schneider, B. Hillebrands, S. O. Demokritov, and M. P. Kostylev, Appl. Phys. Lett. **89**, 063506 (2006).
[9] T. Schneider, A. A. Serga, B. Hillebrands, and M. P. Kostylev, Europhys. Lett. **77**, 57 002 (2007).
[10] V. E. Demidov, S. O. Demokritov, D. Birt, B. O'Gorman, M. Tsoi, and X. Li, Phys. Rev. B **80**, 014429 (2009).